

Residual Entropy of Ordinary Ice from Multicanonical Simulations

Bemd A. Berg^{a,b,c}, Chizuru M ugurum a^d, and Yuko O kam oto^c^{a)} Department of Physics, Florida State University, Tallahassee, FL 32306-4350, USA^{b)} School of Computational Science, Florida State University, Tallahassee, FL 32306-4120, USA^{c)} Department of Physics, Nagoya University, Nagoya, Aichi 464-8602, Japan^{d)} Faculty of Liberal Arts, Chukyo University, Toyota, Aichi 470-0393, Japan

(November 13, 2006)

We introduce two simple models with nearest neighbor interactions on 3D hexagonal lattices. Each model allows one to calculate the residual entropy of ice I (ordinary ice) by means of multicanonical simulations. This gives the correction to the residual entropy derived by Linus Pauling in 1935. Our estimate is found to be within less than 0.1% of an analytical approximation by Nagle which is an improvement of Pauling's result. We pose it as a challenge to experimentalists to improve on the accuracy of a 1936 measurement by Giauque and Stout by about one order of magnitude, which would allow one to identify corrections to Pauling's value unambiguously. It is straightforward to transfer our methods to other crystal systems.

PACS: 61.50.Lt, 65.40.-b, 65.40.Gr, 05.70.-a, 05.20.-y, 2.50.Ng

A thorough understanding of the properties of water has a long history and is of central importance for life sciences. After the discovery of the hydrogen bond [1] it was recognized that the unusual properties of water and ice owe their existence to a combination of strong directional polar interactions and a network of specially arranged hydrogen bonds [2]. The liquid phase of water differs from simple fluids in that there is a large qualitative remnant of ice structure in the form of local tetrahedral ordering [3].

In contrast to liquid water the properties of ice are relatively well understood. Most of them have been interpreted in terms of crystal structures, the forces between its constituent molecules, and the energy levels of the molecules themselves [4,5]. A two-dimensional projection of the hexagonal crystal structure of ordinary ice (ice I) is depicted in Fig. 1 (other forms of ice occur in particular at high pressures). Each oxygen atom is located at the center of a tetrahedron and straight lines (bonds) through the sites of the tetrahedron point towards four nearest-neighbor oxygen atoms. Hydrogen atoms are distributed according to the ice rules [2,6]: (A) There is one hydrogen atom on each bond (then called hydrogen bond). (B) There are two hydrogen atoms near each oxygen atom (these three atoms constitute a water molecule).

In our figure distances are given in units of a lattice constant a , which is chosen to be the edge length of the tetrahedra (this is not the conventional crystallographic definition). For each molecule shown one of the surface triangles of its tetrahedron is placed in the xy -plane. The molecules labeled by u (up) are then at $z = 1/\sqrt{24}$ above, and the molecules labeled by d (down) at $z = -1/\sqrt{24}$ below the xy -plane, at the centers of their tetrahedra. In our computer simulations information about the molecules will be stored in arrays of length N , N being the number of molecules.

Essentially by experimental discovery, extrapolating low temperature calorimetric data (then available down

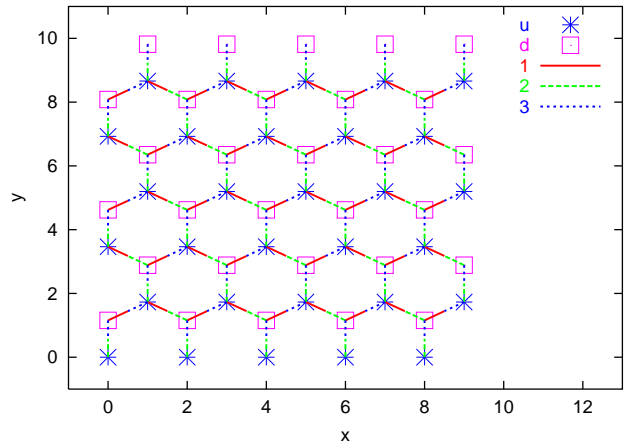


FIG. 1. Lattice structure of one layer of ice I. The up (u) sites are at $z = 1/\sqrt{24}$ and the down (d) sites at $z = -1/\sqrt{24}$. For each site three of its four pointers to nearest neighbor sites are shown.

to about 10 K) towards zero absolute temperature, it was found that ice has a residual entropy [7]:

$$S_0 = k \ln(W) > 0 \quad (1)$$

where W is the number of configurations for N molecules. Subsequently Linus Pauling [6] derived estimates of $W = (W_1)^N$ by two approximate methods, obtaining

$$W_1^{\text{Pauling}} = 3/2 \quad (2)$$

in each case. $W = (W_1)^N$ is the number of Pauling configurations. Assuming that the H_2O molecules are essentially intact in ice, his arguments are:

1. A given molecule can orient itself in six ways satisfying ice rule B. Choosing the orientations of all

molecules at random, the chance that the adjacent molecules permit a given orientation is 1/4. The total number of configurations is thus $W = (6 \cdot 4)^N$.

2. Ignoring condition B of the ice rules, Pauling allows 2^{2N} configurations on the hydrogen bonds between adjacent oxygen atoms: Each hydrogen nucleus is given the choice of two positions, near to one of the two oxygen atoms. At one oxygen atom there are now sixteen arrangements of the four hydrogen nuclei. Of those ten are ruled out by ice rule B. This condition for each oxygen atom permits $6 \cdot 16 = 3 \cdot 8$ of the configurations. Accordingly, the total number of configurations becomes $W = 2^{2N} (3 \cdot 8)^N$.

Equation (2) converts to the residual entropy

$$S_0^{\text{Pauling}} = 0.80574 \text{ cal/deg=mole} \quad (3)$$

where we have used $R = 8.314472 \text{ (15) [J=deg=mole]}$ for the gas constant as of Aug. 20, 2006 given on the NIST website [8] (relying on CODATA 2002 recommended values). This is in good agreement with the experimental estimate

$$S_0^{\text{experimental}} = 0.82 \text{ (5) cal/deg=mole} \quad (4)$$

which was subsequently obtained by Giauque and Stout [9] using refined calorimetry (we give error bars with respect to the last digit(s) in parentheses).

Pauling's arguments omit correlations induced by closed loops when one requires fulfillment of the ice rules for all atoms, and it was shown by Onsager and Dupuis [10] that $W_1 = 1.5$ is in fact a lower bound. Onsager's student Nagle used a series expansion method to derive the estimate [11]

$$W_1^{\text{Nagle}} = 1.50685 \text{ (15)}; \quad (5)$$

or

$$S_0^{\text{Nagle}} = 0.81480 \text{ (20) cal/deg=mole}; \quad (6)$$

Here, the error bar is not statistical but reflects higher order corrections of the expansion, which are not entirely under control. The slight difference between (6) and the value in Nagle's paper is likely due to improvements in the measurements of Avogadro's number [8]. The only independent theoretical value appears to be one for cubic ice, which is obtained by numerical integration of Monte Carlo data [12] and in good agreement with Nagle [11].

Despite Nagle's high precision estimate there has apparently been almost no improvement on the accuracy of the experimental value (4). Some of the difficulties are addressed in a careful study by Haida et al. [13]. But their final estimate remains (4) with no reduction of the error bar. We noted that by treating the contributions in their table 3 as statistically independent quantities and using Gaussian error propagation (instead of adding up

the individual error bars), the final error bar becomes reduced by almost a factor of two and their value would then read $S_0 = 0.815 \text{ (26) cal/deg=mole}$. Still Pauling's value is safely within one standard deviation. Modern electronic equipment should allow for a much better precision. We think that an experimental verification of the difference to Pauling's estimate would be an outstanding confirmation of structures imposed by the ice rules.

In this paper we provide a novel high-precision numerical estimate of S_0 for ordinary ice. Our calculations are based on two simple statistical models, which reflect Pauling's arguments. Each model is defined on the hexagonal lattice structure of Fig. 1.

In the first model, called 6-state H_2O molecule model, we allow for six distinct orientations of each H_2O molecule and define its energy by

$$E = \sum_b h(b; s_b^1; s_b^2); \quad (7)$$

Here, the sum is over all bonds b of the lattice and $(s_b^1$ and s_b^2 indicate the dependence on the states of the two H_2O molecules, which are connected by the bond)

$$h(b; s_b^1; s_b^2) = \begin{cases} 1 & \text{for a hydrogen bond;} \\ 0 & \text{otherwise;} \end{cases} \quad (8)$$

In the second model, called 2-state H-bond model, we do not consider distinct orientations of the molecule, but allow two positions for each hydrogen nucleus on the bonds. The energy is defined by

$$E = \sum_s f(s; b_s^1; b_s^2; b_s^3; b_s^4); \quad (9)$$

where the sum is over all sites (oxygen atoms) of the lattice. The function f is given by

$$f(s; b_s^1; b_s^2; b_s^3; b_s^4) = \begin{cases} 2 & \text{for two hydrogen nuclei close to } s; \\ 1 & \text{for one or three hydrogen nuclei close to } s; \\ 0 & \text{for zero or four hydrogen nuclei close to } s; \end{cases} \quad (10)$$

The groundstates of each model fulfill the ice rules. At $T = 0$ the number of configurations is 6^N for the 6-state model and 2^{2N} for the 2-state model. Because the normalizations at $T = 0$ are known, multicanonical (MUCA) simulations [14] allow us in either case to estimate accurately the number of groundstate configurations [15]. Superficially both systems resemble Potts models (see, e.g., [16] for Potts model simulations), but their thermodynamic properties are entirely different. For instance, we do not find any sign of a disorder-order phase transition, which is for our purposes advantageous as the MUCA estimates for the groundstate entropy become particularly accurate. This absence of a bulk transition does not rule out long-range correlations between bonds of the groundstate configurations, which are imposed by the conservation of the flow of hydrogen bonds at each molecule. In that sense the ground state is a critical ensemble.

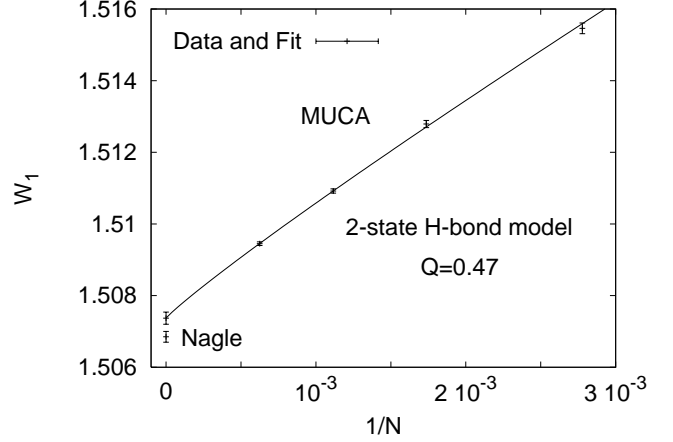
TABLE I. Simulation data for W_1 .

N	n_x	n_y	n_z	6-state model		2-state model		Q
				W_1	N_{cyc}	W_1	N_{cyc}	
128	4	8	4	1:52852 (47)	1854	1:52869 (23)	7092	0.72
360	5	12	6	1:51522 (49)	223	1:51546 (15)	1096	0.65
576	6	12	8	1:51264 (18)	503	1:51279 (10)	1530	0.47
896	7	16	8	1:51075 (16)	208	1:51092 (06)	2317	0.32
1600	8	20	10	1:50939 (09)	215	1:50945 (05)	619	0.56
1 (t)				1:50741 (33)		1:50737 (17)		0.91

Using periodic boundary conditions (BCs), our simulations are based on a lattice construction set up earlier by one of us [17]. Following closely the method outlined in chapter 3.1.1 of [16] four index pointers from each molecule to the array positions of its nearest neighbor molecules are constructed. The order of pointers one to three is indicated in Fig. 1. The fourth pointer is up the z-direction for the u molecules and down the z-direction for the d molecules. The lattice contains then $N = n_x n_y n_z$ molecules, where n_x , n_y , and n_z are the number of sites along the x, y, and z axes, respectively. The periodic BCs restrict the allowed values of n_x , n_y , and n_z to $n_x = 1; 2; 3; \dots$, $n_y = 4; 8; 12; \dots$, and $n_z = 2; 4; 6; \dots$. Otherwise the geometry does not close properly. Using the inter-site distance $r_{00} = 2.764 \text{ \AA}$ from Ref. [5], the physical size of the box is obtained by putting the lattice constant a to $a = 2.257 \text{ \AA}$, and the physical dimensions of the box are calculated to be $B_x = 2n_x a$, $B_y = (n_y - 3 = 2)a$, $B_z = (n_z - 6)a$. In our choices of n_x , n_y , and n_z values we aimed within reasonable limitations at symmetrically sized boxes.

Table I compiles our MUCA W_1 estimates for the lattice sizes used. In each case a Wang-Landau recursion [18] was used to estimate the MUCA parameters for which besides a certain number of cycling events [16] a flatness of $H_{min} = H_{max} > 0.5$ was considered sufficient for stopping the recursion and starting the second part of the MUCA simulation with fixed weights ($H(E)$ is the energy histogram, H_{min} is the smallest and H_{max} the largest number of entries in the flattened energy range).

The statistics we used for measurements varied between $32 \cdot 10^6$ sweeps for our smallest and $64 \cdot 10^7$ sweeps for our largest lattice. Using two 2 GHz PCs the simulations take less than one week. The number of cycles, N_{cyc} , completed between $m_{in} = 0$ and the groundstate are listed in the 6-state and 2-state model columns of table I. As each of our simulations includes the $m_{in} = 0$ canonical ensemble, the (logarithmically coded) re-weighting procedure of chapter 5.1.5 of [16] delivers estimates for W_1 , which are compiled in the same columns. Each error bar relies on 32 jackknife bins. As expected, the values from both models are consistent as is demonstrated by Q values of Gaussian difference tests (see, e.g., chapter 2.1.3 of [16]) in the last column of the table. The 2-state H-bond model gives more accurate estimates than the 6-state H_2O molecule model, obviously


 FIG. 2. Fit for W_1 .

by the reason that the cycling time, which is $1/N_{cyc}$, is less for the former, because the energy range that needs to be covered is smaller.

In Fig. 2 a fit for the data of the 2-state H-bond model to the form

$$W_1(x) = W_1(0) + a_1 x ; \quad x = 1/N \quad (11)$$

is shown. The $W_1 = W_1(0)$ estimate from Fig. 2 is given in the the last row of the 2-state model column of table I. The data point for the smallest lattice is included in the fit, but not shown in the figure where we like to focus on the large N region. The goodness of fit (chapter 2.8 of [16]) is $Q = 0.47$ as given in the figure. Similarly the estimate for the 6-state H_2O molecule model in the last row of the table is obtained with a goodness of fit $Q = 0.78$. All Q values (Gaussian difference tests and fits) are in the range one would expect for statistically consistent data. The values of the fits were also consistent and their combined value is $\chi^2 = 0.923$ (23). That we have $\chi^2 \approx 1$ reflects bond correlations in the groundstate ensemble.

Combining the two fit results weighted by their error bars leads to our final estimate

$$W_1^{MUCA} = 1:50738 (16) : \quad (12)$$

This converts into

$$S_0^{MUCA} = 0:81550 (21) \text{ cal/deg/mole} : \quad (13)$$

for the residual entropy.

The difference between (12) and the estimate of Nagle (5) is 0.035% of the estimated W_1 value (0.086% of S_0), which is much smaller than any foreseeable experimental error. However, within their own error bars the Gaussian difference test between the two estimates yields $Q = 0.016$. As the error bar in (12) covers and no systematic errors due to finite size corrections from larger lattices, the small discrepancy with Nagle's result may

well be explained this way. In view of the large error bar in the experimental estimate it appears somewhat academic to trace the ultimate reason.

As already (hesitatingly) pointed out by Pauling [6], the real entropy at zero temperature is not expected to agree with the residual entropy extrapolated from low but non-zero temperatures. In real ice one expects a small splitting of the energy levels of the Pauling configurations, which are degenerate in both of our models. Once the thermal fluctuations become small compared with these energy differences, the entropy will become lower than the residual entropy calculated here. Such an effect is observed in [13] by annealing ice I at temperatures between 85 K and 110 K. Refined models are needed to gain computational insights. Crossing this temperature range sufficiently fast allows one still to extract the residual entropy, because the relaxation time has become so long that one does not have ordering of Pauling states during typical experimental observation times.

It is clear that our method carries rather easily over to other crystal structures for which one may want to calculate residual entropies. In particular structural defects and impurities can be included, although one may have to use more realistic energy functions and lattice sizes put limits on low densities. Simulations very similar to those performed here should enable accurate estimates of the residual entropies for other forms of ice and various geometrically frustrated systems [19] as well as for spin models in the class for which lower bounds on their residual entropies were derived in [20]. For more involved systems our approach is to design simple models, which share the relevant groundstate symmetries with the system of interest. That could, for instance, have applications to the residual entropy of proteins by allowing for more realistic modeling than done in Ref. [21].

Finally, good modeling of water is of crucial importance for computational progress in biophysics. Clusters of hydrogen bonds play a prominent role in water at room temperature. Our method allows one to calculate the combinatorial factors W_1^N with which small clusters ought to be calculated in phenomenological water models like those discussed in Ref. [3]. Through a better understanding of hydrogen bond clusters insights derived from the study of ordinary ice may well be of importance for improving on models [22], which have primarily been constructed to reflect properties of water under room temperatures and pressures.

ACKNOWLEDGMENTS

We like to thank John Nagle for e-mail comments on the first version of this paper. During most of this work Bernd Berg was supported by a fellowship of the JSPS. Chizuru MUGURUMA and Yuko OKAMOTO were supported, in part, by the Ministry of Education, Culture, Sports, Science and Technology (MEXT), Japan:

Chizuru MUGURUMA by Grants-in-Aid for Young Scientists (B), Grant No. 16740244 and Yuko OKAMOTO by Grants-in-Aid for the Next Generation Super Computing Project, Nanoscience Program and for Scientific Research in Priority Areas, Water and Biomolecules.

-
- [1] W. M. Latimer and W. H. Rodebush, *J. Am. Chem. Soc.* **42**, 1419 (1920).
 - [2] J. D. Bernal and R. H. Fowler, *J. Chem. Phys.* **1**, 515 (1933).
 - [3] H. S. Frank and W. -Y. Wen, *Discussions Faraday Soc.* **24**, 133 (1957); G. Nemethy and H. A. Scheraga, *J. Chem. Phys.* **36**, 3382 (1962); F. Sciortino, A. Geiger, and H. E. Stanley, *J. Chem. Phys.* **96**, 3857 (1992).
 - [4] D. Eisenberg and W. Kauzmann, *The Structure and Properties of Water*, Oxford University Press, Oxford 1969.
 - [5] V. F. Petrenko and R. W. Whitworth, *Physics of Ice*, Oxford University Press, Oxford 1999.
 - [6] L. Pauling, *J. Am. Chem. Soc.* **57**, 2680 (1935).
 - [7] W. F. Giauque and M. Ashley, *Phys. Rev.* **43**, 81 (1933).
 - [8] National Institute of Standards and Technology (NIST) at <http://physics.nist.gov/cuu/>.
 - [9] W. F. Giauque and J. W. Stout, *J. Am. Chem. Soc.* **58**, 1144 (1936).
 - [10] L. Onsager and M. Dupuis, *Re. Scu. Int. Fis. Enrico Fermi* **10**, 294 (1960).
 - [11] J. F. Nagle, *J. Math. Phys.* **7**, 1484 (1966).
 - [12] S. V. Isakov, K. S. Ramani, R. M. Oessner, and S. L. Sondhi, *Phys. Rev. B* **70**, 104418 (2004).
 - [13] O. Haida, T. Matsuo, H. Suga, and S. Seki, *J. Chem. Thermodynamics* **6**, 815 (1974).
 - [14] B. A. Berg and T. Neuhaus, *Phys. Rev. Lett.* **68**, 9 (1992).
 - [15] B. A. Berg and T. Celik, *Phys. Rev. Lett.* **69**, 2292 (1992).
 - [16] B. A. Berg, *Markov Chain Monte Carlo Simulations and Their Statistical Analysis*, World Scientific, Singapore, 2004.
 - [17] B. A. Berg, 2005 (unpublished).
 - [18] F. Wang and D. P. Landau, *Phys. Rev. Lett.* **86**, 2050 (2001).
 - [19] R. Higashinakawa, H. Fukazawa, K. Degushi, and Y. Maeno, *J. Phys. Soc. Japan* **73**, 2845 (2004) and references given therein.
 - [20] Y. Chow and F. Y. Wu, *Phys. Rev. B* **36**, 285 (1987).
 - [21] Z. Li, S. Raychaudhuri, and A. J. Wand, *Protein Science* **5**, 2647 (1996).
 - [22] See references collected in C. Vega, E. Sanz, and J. L. F. Abascal, *J. Chem. Phys.* **122**, 114507 (2005).